Optoelectronic transport property measurements of an amorphous-silicon-passivated c-silicon wafer using non-contacting methodologies

A. Melnikov [a],*, B. Halliop [b], A. Mandelis [a,b], N.P. Kherani [b]

[a] Center for Advanced Diffusion-Wave Technologies (CADIFT), Department of Mechanical and Industrial Engineering, University of Toronto, Toronto, ON, M5S 3G8, Canada
[b] Electrical and Computer Engineering, University of Toronto, Toronto, ON, M5S 3G4, Canada

ARTICLE INFO

ABSTRACT

Photocarrier radiometry (PCR), microwave photoconductivity decay (μ-PCD) and transient and quasi-steady-state eddy currents were used for the characterization of a crystalline (c-) Si wafer passivated with intrinsic hydrogenated amorphous silicon films on either front or back side, or on both sides of the wafer. All three techniques are capable of measuring recombination lifetimes, however additional fundamental free photoexcited carrier transport parameters (diffusion coefficient, front- and back-surface recombination velocity) can be evaluated from the PCR frequency dependence owing to the free-carrier-density wave's diffusion-length depth-dependence on frequency. The measured recombination lifetimes are compared and differences in values among the three techniques are discussed in terms of the role of surface and interface defects. μ-PCD and eddy currents yield effective or vertically averaged lifetime measurements, as opposed to PCR which yields bulk recombination lifetimes separately from surface recombination effects.

© 2012 Elsevier B.V. All rights reserved.

1. Introduction

Carrier lifetime and interface defect density are major efficiency impacting parameters for high-efficiency photovoltaics. In the case of high-quality crystalline materials, the bulk recombination rate is very low and surface recombination dominates the effective recombination lifetime. Therefore, efficient passivation of interface defects is of great interest. One such passivating material is amorphous (α-) silicon which can also be doped and can form a heterojunction solar cell. The amorphous-crystalline-silicon *p-n* heterojunction is a paradigm shift compared to more traditional thermally diffused junctions. The nano-thin hydrogenated amorphous silicon layer provides excellent passivation allowing conversion efficiency increase of more than 22% [1], while its low temperature (~200 °C) synthesis presents a cost advantage. Study of this type of device is of considerable interest.

Photocarrier radiometry (PCR) was first introduced in studies of crystalline Si wafers as a quantitative dynamic form of spectrally-gated photoluminescence (PL) [2,3] in which thermal mid-infrared photon (Planck) emissions, the result of superband-gap photon absorption and temperature rise due to non-radiative (thermal) recombination of photo-excited carriers (defined as photothermal radiometry, PTR) [4] are spectrally gated out. PCR is a process complementary to PTR, arising in purely radiative-recombination-induced near-infrared emission signals which are collected and detected with a suitable near-infrared photodetector. PCR yields quantitative information about transport and radiative recombination processes in semiconductors. In silicon it can be used through a modulation frequency scan for the simultaneous extraction of all four fundamental electronic transport parameters: bulk lifetime, ambipolar diffusion coefficient, and back- and front-surface recombination velocities. Along with conventional non-contacting methods, such as quasi-steady-state and transient eddy current detection and photoconductance, which use microwave reflectance, modulated PL has been used in recent years for the determination of the effective carrier lifetime of an amorphous-silicon passivated c-Si and α-silicon/c-Si heterojunction solar cell [5–7]. The effective lifetime was extracted from the phase measurement for the case of a homogeneous carrier distributions. The effective lifetime is usually defined as the inverse of the sum of recombination rates in the bulk and at the front and back surfaces. Consequently, the effective lifetime is sensitive to the quality of these two surfaces. However, the simultaneous determination of all four transport parameters remains difficult, especially in case of inhomogeneous distributions of excess minority carriers. Carrier distribution inhomogeneity is higher for thin wafers with high values of, or combinations of large differences between, front- and back-surface recombination velocities, significant concentrations of defects (traps), and/or high absorption coefficients of the excitation radiation leading to very steep photocarrier axial concentration gradients. The frequency-scanned PCR technique is dynamic and therefore capable of providing the aforementioned measurements over a wide range of modulation frequencies for materials and devices exhibiting large carrier distribution inhomogeneities such as combinations of passivated and unpassivated surfaces. Conventional static (DC) optoelectronic transport measurement methodologies lump bulk and surface recombination rates into one effective lifetime because they are insensitive or

* Corresponding author.
 E-mail address: melnikov@mie.utoronto.ca (A. Melnikov).

unable to resolve large differences of these properties across the bulk and opposite surfaces of substrates and devices.

In this paper the PCR technique is used for the determination of electronic transport parameters of a hydrogenated α-silicon-passivated crystalline silicon wafer. Comparison of the PCR-extracted lifetimes with those evaluated with microwave photoconductive decay, and transient and quasi-steady-state eddy current measurements is presented.

2. Experimental details

The sample examined consisted of a *n*-type silicon wafer divided into four sections using masks. The substrate was a 290-μm thick, 1 Ω cm CZ silicon wafer, onto which intrinsic hydrogenated amorphous silicon (i-α-Si:H) films were deposited by DC saddle field plasma enhanced chemical vapor deposition (DCSF-PECVD), at 170 °C. The DC saddle field is an adaptation that provides some of the benefits of an RF system and some of the benefits of a DC system. In the case of a DCSF-PECVD system, a DC cathode is sandwiched between two grounded anodes, with the substrate positioned beyond one of the anodes. This field allows ions to oscillate around the cathode, extending their mean free path and thus allowing the system to sustain stable plasma at lower pressures than in a DC diode system. Secondly, it isolates the substrate from the plasma, reducing ion bombardment on the substrate. Carrier lifetimes as high as 5 ms have been reported using this method to passivate silicon wafers.

A mask was used to cover half of the wafer while a 30-nm-thick i-α-Si:H film was deposited on the front surface. Then the wafer was turned over to expose the back surface and the mask was rotated 90 degrees to deposit a 30-nm thick i-α-Si:H film on the back. In this manner four distinct areas were fabricated on the wafer depending on whether the front, back, neither, or both were masked during deposition.

3. Carrier transport property measurements and imaging

The PCR system has been described elsewhere [8] and a schematic is shown in Fig. 1. An 830-nm diode laser internally modulated using the voltage output from a function generator is used as a carrier excitation source. A gradium lens is used to focus the laser beam onto the sample surface coincident with the focal point of an off-axis paraboloidal mirror that collects a portion of any diffuse backscattered photons. The collected light is then focused onto an InGaAs detector with a switchable gain preamplifier built into the detector housing and a frequency response of up to 10 MHz. The detector has a spectral bandwidth of 800–1750 nm (0.71–1.55 eV) with a peak response at 1550 nm and an active element with a 1-mm diameter. The system is designed such that the specular reflection of the excitation beam is not collected by the paraboloidal mirrors and thus is not focused onto the detector. This allows for the collection of near-IR recombination photons from the bulk of the sample and not specularly from the surface. A long-pass filter with a steep cut-on and a transmission range of 1042–2198 nm is placed in front of the detector in order to ensure that any diffuse reflections of the excitation source do not contribute to the signal. The signal from the detector is demodulated by a lock-in amplifier. The sample holder is connected to a motorized X–Y stage assembly to allow for sample positioning and imaging, and a third stage in the vertical direction is used to manually adjust the sample to the focal point of the collection optics. All instruments, data acquisition, and lateral sample positioning are controlled using a MATLAB program.

PCR frequency-scan measurements from 10 Hz to 100 kHz with focused laser beam were carried out at room temperature using square-wave modulation of the laser intensity. The spotsize on the silicon wafer and the output power of the laser were approx. 500 μm, and 27.4 mW, respectively. For point-by-point scanning imaging the silicon wafer was irradiated with the focused laser beam at a fixed modulation frequency leading to high-frequency PCR images, or at fixed coordinate points leading to PCR frequency scans. For standard lifetime measurements using eddy current, a wide spectrum light source was employed and two different measurement methods were used, depending on lifetime values. The transient method was used for longer lifetimes (above approximately 200 μs), while for shorter lifetimes a quasi-steady state method was employed. Light intensity was controlled so as to create a carrier density of 10^{15} cm^{-3}. The lifetime measurements via eddy current were performed with a Sinton Instruments model WCT-120. Microwave reflectance PCD (μ-PCD) measurements were performed with a Semilab WT-2000 system using a 904 nm laser and a microwave frequency of 10 GHz.

According to PCR theory [2,3], the signal depends mainly on the minority carrier-density-wave (CDW) lifetime, the ambipolar diffusion coefficient, and front-surface and back-surface (to a lesser extent) recombination velocities. Signal amplitude and phase are
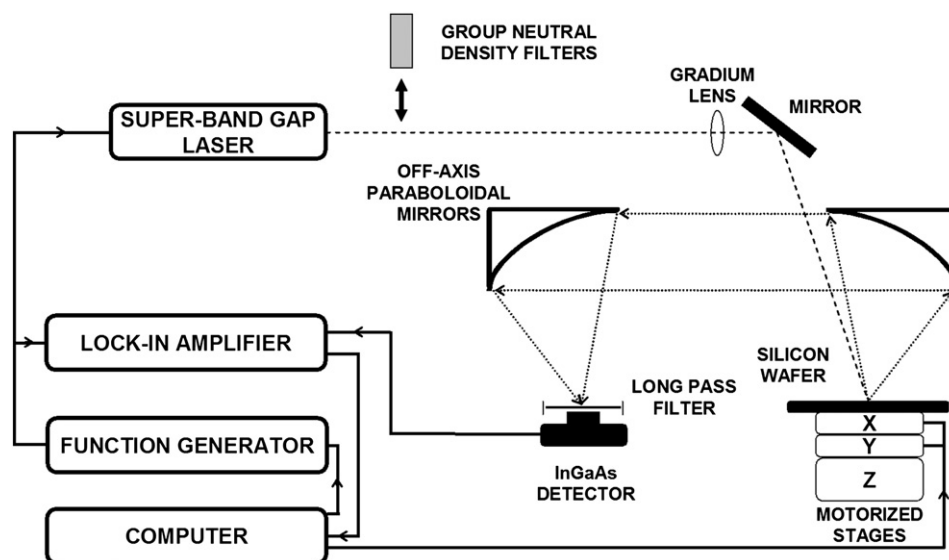

Fig. 1. Schematic diagram of experimental PCR system.

determined by the magnitude and depth of the free CDW centroid integral, respectively:

$$S(\omega) \approx F(\lambda_1, \lambda_2) \int_0^L \Delta N(z, \omega) dz \qquad (1)$$

where F is a function of the spectral bandwidth (λ_1, λ_2) of the IR detector; $\Delta N(z,\omega)$ is the optically generated excess free-CDW at depth z, L is wafer thickness and ω is the angular modulation frequency. The free-CDW depends on ac carrier diffusion length $L_e(\omega)$

$$L_e(\omega) = \sqrt{\frac{D^*\tau}{1 + i\omega\tau}} \qquad (2)$$

where D^* is the ambipolar carrier diffusion coefficient and τ is the minority recombination (bulk) lifetime. In order for back surface recombination to influence the PCR signal, the relation between L_e and L must be: $L_e \geq L$.

PCR frequency scans of the passivated c-Si wafer on both, either or neither side (unpassivated) are presented in Fig. 2. The dependencies of PCR amplitude clearly show an increasing CDW amplitude integral for passivated back side, front side, and more than 3 orders of magnitude for two-side passivation. The trends confirm the significant influence of i-α-Si/c-Si interface defect concentration at both front- and back-side interfaces on the concentration of excess minority carriers, although carrier generation takes place only near the front surface, essentially within the optical absorption length. On turning the wafer over, essentially the same dependencies are obtained for the same depthwise configurations. It is worth mentioning that the PCR dependencies on non-passivated and back-side passivated surfaces coincide above approx. 50 kHz in both amplitude and phase, Fig. 2, a fact indicating the frequency threshold above which the carrier diffusion wave does not reach the back surface for this configuration.

Multi-parameter 3-D best fits according to PCR theory [2,3] have been described elsewhere [9]. The results of applying the best-fitting procedure to the data of Fig. 2 are presented in Table 1. The Table also shows the results of minority carrier lifetime measurements from the μ-PCD and from the transient and quasi-steady-state (QSS) eddy current methods. Overall, the PCR bulk lifetimes exhibit the same trends as those evaluated from the alternative measurements (Table 1 and Fig. 3). Smaller values of PCR lifetimes correspond to smaller values of effective lifetimes measured by the conventional techniques; the same is true for longer values. However, Table 1 shows that PCR bulk lifetimes for the one-side passivated case or with no passivation are significantly higher than those evaluated from the photoconductivity and Eddy current methods. Furthermore, there is no agreement between μ-PCD and Eddy current lifetime measurements in the unpassivated and back-side passivated configurations. These differences are related to the physical processes used by each methodology to measure lifetimes. They may occur because the μ-PCD method does not separate out bulk and surface recombination lifetimes and/or from the different excitation wavelengths
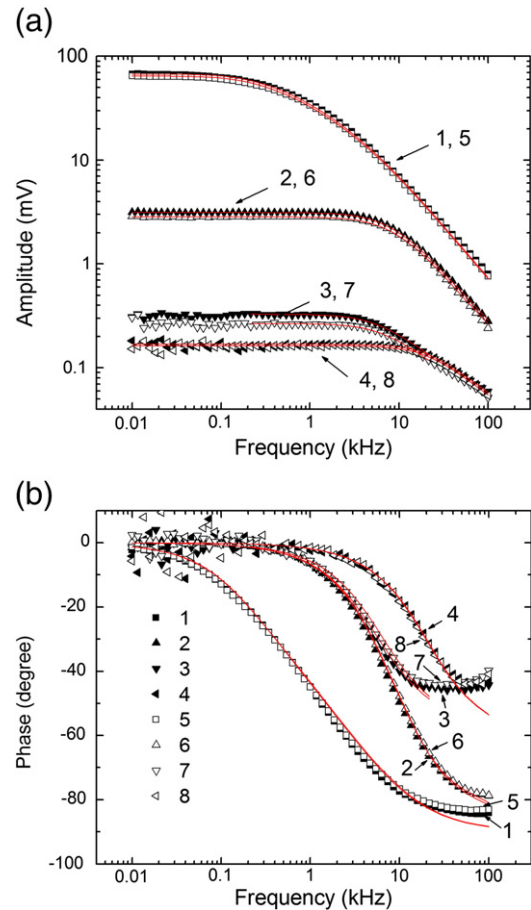

Fig. 2. PCR frequency dependence of c-Si wafer with passivation both-, front,- or back-side by i-α-Si, or without passivation. Measurements were carried out on both sides of the wafer with 0.5 mm 27.4 mW laser beam spotsize: 1 — α-Si on front and back sides, 2 — α-Si on front side, 3 — α-Si on back side, 4 — unpassivated, 5 — α-Si on front and back sides with wafer flipped over, 6 — α-Si on front side for flipped-over wafer, 7 — α-Si on back side of flipped-over wafer, 8 — unpassivated for flipped-over wafer. Solid line — theoretical fit. a) Amplitude, b) phase.

and generally different manner in which lifetime affects each measurement. On the other hand, PCR bulk lifetimes are measured separately from the effects of surface recombination. For the case of both passivated sides (measured from both sides), when surface recombination velocities on both sides are small, the measured PCR and Eddy current lifetimes are much longer than the μ-PCD values. This is expected from PCR, as it yields a bulk lifetime separate from the inverse surface recombination rate (surface lifetime equivalent). It is important to note that changes incurred

Table 1

Measured lifetime and best fitted transport parameters of passivated and non-passivated c-Si: bulk lifetime τ_B, ambipolar diffusivity D, front surface recombination S_1 and back surface recombination S_2.

| α-Si passivation layers	μ-PCD measurements	Eddy current measurements	PCR			
	τ (μs)	τ (μs)	τ_B (μs)	D (cm²/s)	S_1 (cm/s)	S_2 (fixed) (cm/s)
Front and back	718	1379.7 (transient)	1036	3.1	1.8	0.5
Front only	34.4	33 (QSS)	206	5.3	3.8×10^2	1.7×10^5
Back only	30.9	7.6 (QSS)	203	4.0	5.4×10^6	3.2×10^2
None	8.3	3.5 (QSS)	19	7.2	1.7×10^5	4.0×10^4
Front and back (wafer flipped over)	660.1	1390.8 (transient)	1051	3.2	1.3	0.4
Front only (wafer flipped over)	33.9	33 (QSS)	146	5.6	3.2×10^2	1.7×10^5
Back only (wafer flipped over)	31.1	7.2 (QSS)	95	3.8	3.4×10^6	3.8×10^2
None (wafer flipped over)	8.3	3.5 (QSS)	21	7.3	1.7×10^5	3.8×10^4
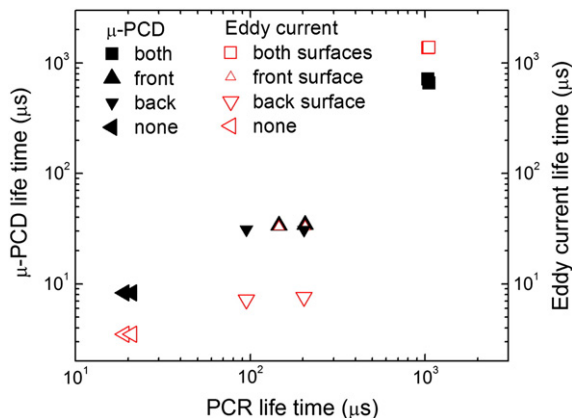
Fig. 3. Correlation among lifetimes evaluated with three methods (data from Table 1).

in the electronic quality of the surfaces through passivation greatly affect the bulk lifetime values. The transient Eddy current lifetime values of the front- and back-passivated wafer are approx. 30% higher than the PCR values. While there is no clear explanation for this difference, it is possible that the simple Eddy current measurement algorithm ignores higher eigenvalue contributions to the overall transient [10] which would decrease the actual value of the fundamental (longest) decay time. The large variations in the PCR measured bulk lifetimes in Table 1 and their anti-correlations with surface recombination velocities can be under-stood in the light of well-known recombination mechanisms. In the Shockley-Read picture of free-carrier statistics in the presence of bandgap traps [11], bulk lifetime depends on photocarrier injection level [12]: With increasing optical injection level traps become filled up and free-carrier capture probability decreases, thereby increasing the effective bulk recombination lifetime, τ_B. Due to the short optical absorption length in Si at 830 nm S_1 greatly affects the net excess CDW: decreased S_1 acts like increased injection rate which results in a correspondingly increased bulk lifetime. It is known that irradiation of the surface with an additional DC optical source affects the value of S_1 and results in changes in the effective recombination lifetime [13,14]. These trends are also amply exhibited in the relative τ_B values of Table 1. In contrast, unlike the situation with trap- and surface-sensitive bulk recombination lifetimes, the value of the intrinsic bulk lifetime across the substrate wafer is set by the doping density. It is substantially insensitive to donor concentration for doping densities $<10^{16}$ cm^{-3} and depends mainly on the amount of crystal-growth impurities [15]. For higher doping densities both n- and p-type substrate lifetimes decrease with increasing doping density. This mechanism is expected to be active across the entire wafer regardless of surface condition changes as a result of device processing [15]. However, even in this situation, it has been found that the dependence of the screening length on carrier concentration affects the variation of bulk lifetime with doping density [16].

Along with bulk lifetimes, the front- and back-surface recombina-tion velocity and ambipolar diffusion coefficient were evaluated from PCR frequency dependencies (Table 1). Best fits were obtained with fixed back-surface recombination velocity which was chosen such that differences between front- and back-surface velocities, respec-tively, for depthwise symmetrical structures on the wafer (both sides passivated or both unpassivated) were minimized as a result of simultaneous best fitting of amplitudes and phases and obtaining the square deviation minimum. Owing to the lower PCR sensitivity to back-surface recombination velocity under asymmetric surface recombination configurations, the back-surface recombination veloc-ity for non-symmetric wafer structures was chosen according to the best-fitted results obtained from the same structures in the respective symmetric configurations. It is important to note all four transport parameter measurements, lifetime, surface recombination velocities

and ambipolar diffusion coefficient show a dependence on the excess minority carrier concentration, as expected [17–22]. As discussed above, a decrease in surface recombination velocity by passivation of the i-α-Si structure leads to an increase of excess minority carrier concentration, resulting in significant increase of the PCR amplitude. The effective CDW bulk recombination lifetime clearly increases with passivation (effective higher injection rate). The lifetime of the front-side passivated structure measured using Eddy current is similar to that measured with μ-PCD, yet it is much higher than that of the back-side passivated structure measured by Eddy current, whereas there is little difference between μ-PCD lifetimes of the two structures. This Eddy-current lifetime difference is the consequence of the large inhomogeneity of excess carrier depth generation by the broad-spectrum light source used in the Eddy current method, since carriers are generated mainly near the front surface unlike with μ-PCD. The PCR lifetimes are similar for both surfaces, as expected from a method that measures bulk lifetime values based not on the optical distribution, but on the diffusion-wave following very-near-surface illumination from either side. They are longer than μ-PCD lifetimes as they do not average out the bulk and surface contributions. In Table 1, the ambipolar diffusion coefficient, D, is minimum in the case of highest CDW (front- and back-surface passivation) due to the decrease in carrier mobility as a consequence of carrier-carrier scattering [23,24]. Consistently, D is maximum in the case of lowest CDW (non-passivation). Surface recombination velocity for i-α-Si/c-Si interfaces measured using PCR is much smaller for the two-side passivated structure than those for one-side passivation. This effect may be caused by excess photocarrier-mediated charged-surface-defect occupation and neutralization owing to the significantly higher photo-excited carrier bulk CDW present in the wafer structure which is passivated on both sides. The surface recombination velocity is known to demonstrate strong dependence on minority excess carrier concentration [21,22].

Fig. 2 shows large deviations from the theoretical best fit for phase frequency dependencies above 20–50 kHz: the experimental phase lag saturates, while the theoretical lag continues to increase. This effect is especially clear for the configuration with the back side passivated or unpassivated. The high-frequency phase lag saturation may be due to uncompensated charge at the interface [14]. The effective surface charge sink tends to confine the CDW centroid [2] closer to the surface resulting in a smaller phase lag than that of a compensated surface. While it is well-known that silicon oxide can store uncompensated charge, the nature of the charged i-α-Si/c-Si interface remains unclear. It should be noted that the high-frequency amplitudes in Fig. 2(a) are less sensitive to surface charging phenomena because the bulk CDW dominates the PCR signal.

Fig. 4 shows point-by-point laser scanned PCR images at 100 Hz, 5 kHz, and 100 kHz obtained near the center of the same wafer used to generate the results of Fig. 2. By choosing this region, laser PCR scanning was able to cross all 4 configurations as indicated in Fig. 4a. All images confirm a high degree of homogeneity of the i-α-Si/c-Si interface. At high frequencies (~100 kHz), where the CDW does not reach the back-surface ("electronically thick"), areas with and without passivated backside have similar PCR amplitude and phase, in agreement with Fig. 2. These images demonstrate that PCR imaging is depth profilometric and can yield CDW information down to subsurface depths determined by the modulation frequency and the ac carrier diffusion length.

4. Conclusions

In conclusion, detailed comparisons of the PCR-derived bulk lifetime values with those obtained using microwave photoconductivity decay and transient and quasi-steady-state Eddy current measurements were made on an amorphous-silicon-passivated c-silicon wafer. The similar lifetime trends with surface processing among all three techniques, albeit not leading to equal lifetimes or direct proportionalities among
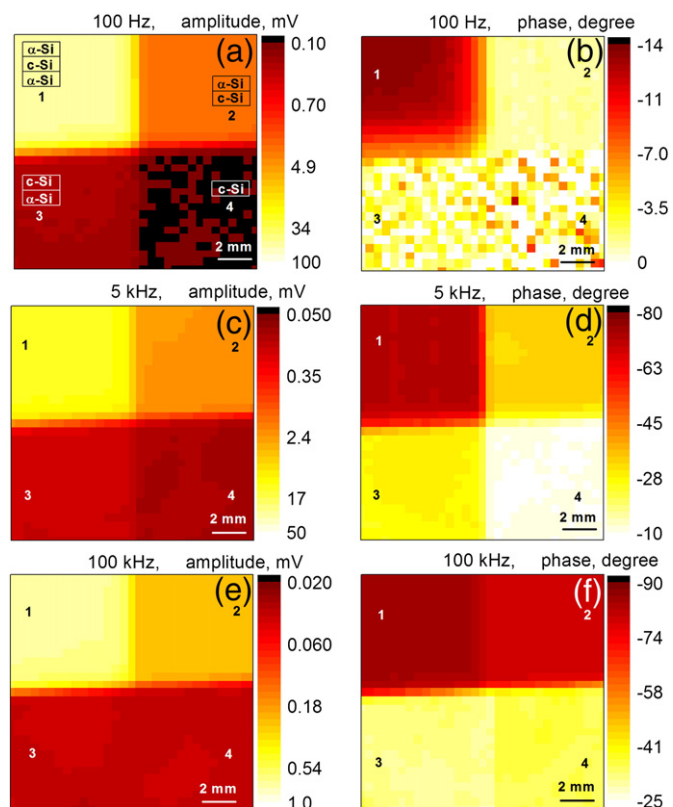
Fig. 4. Lock-in point-by-point amplitude and phase images at 100 Hz (a, b), 5 kHz (c, d), and 100 kHz (e, f). Images were constructed using focused laser beam scans with 0.5 mm step and 0.5 mm spotsize.

occupation of bandgap traps under variable optical injection rates as expected, e.g., in photovoltaic solar-cell applications. PCR measurements were found to yield longer bulk lifetime values than the other methodologies for single-surface passivation or no passivation, because this method is capable of separating out bulk lifetime from surface recombination lifetimes. Effective lifetimes as measured by the other methods, however, cannot differentiate between bulk and surface and yield an *effective combined* lifetime [10,17]. As a result the additional transport parameter information available with the PCR method shows excellent potential for quantitative optoelectronic quality control of the i-α-Si/c-Si interface in surface processed Si wafers.

Acknowledgments

References

[1] Y. Tsunomura, Y. Yoshimine, M. Taguchi, T. Baba, T. Kinoshita, H. Kanno, H. Sakata, E. Maruyama, M. Tanaka, Sol. Energy Mater. Sol. Cells 93 (2009) 670.
[2] A. Mandelis, Diffusion-Wave Fields: Mathematical Methods and Green Functions, Springer, New York, 2001 Chap. 9.
[3] A. Mandelis, J. Batista, D. Shaughnessy, Phys. Rev. B 67 (2003) 205208.
[4] T. Ikari, A. Salnick, A. Mandelis, J. Appl. Phys. 85 (1999) 7392.
[5] K.R. Leong, A. Mandelis, N.P. Kherani, S. Zukotynski, MRS Symp. Proc. vol. 910 (2006) A06.
[6] R. Brüggemann, S. Reynolds, J. Non-Cryst. Sol. 352 (2006) 1888.
[7] R. Brüggemann, J. Opt. Dev. Adv. Mat. 11 (2009) 1072.
[8] D. Shaughnessy, A. Mandelis, J. Electrochem. Soc. 153 (2006) G283.
[9] B. Li, D. Shaughnessy, A. Mandelis, J. Appl. Phys. 97 (2005) 023701.
[10] K.L. Luke, L.J. Cheng, J. Appl. Phys. 61 (1987) 2282.
[11] W. Shockley, W.T. Read Jr., Phys. Rev. 87 (1952) 835.
[12] W.M. Bullis, H.R. Huff, J. Electrochem. Soc. 143 (1996) 1399.
[13] A. Mandelis, J. Batista, J. Gibkes, M. Pawlak, J. Pelzl, J. Appl. 97 (2005) 083507.
[14] A. Mandelis, J. Appl. Phys. 97 (2005) 083508.
[15] L. Passari, E. Susi, J. Appl. Phys. 54 (1983) 3935.
[16] K. Betzler, R. Conradt, Solid State Commun. 17 (1975) 823.
[17] D.K. Schroder, Semiconductor Material and Device Characterization, Sec. ed. John Wiley & Sons, 1998.
[18] A. Melnikov, A. Mandelis, J. Tolev, P. Chen, S. Huq, J. Appl. Phys. 107 (2010) 114513.
[19] R. Gogolin, N.-P. Harder, R. Brendel, Photovoltaic Specialists Conference (PVSC), 2010 35th IEEE, 2010, p. 443.
[20] J. Brody, A. Rohatgi, Solid State Electron. 45 (2001) 1549.
[21] A.G. Aberle, S. Glunz, W. Warta, J. Appl. Phys. 71 (1992) 4422.
[22] T. Lauinger, J. Schmidt, A.G. Aberle, R. Hezel, Appl. Phys. Lett. 68 (1996) 1232.
[23] J.M. Dorkel, P. Leturgo, Solid State Electron. 24 (1981) 821.
[24] C.-M. Li, T. Sjodin, H.-Lung Dai, Phys. Rev. B 56 (1997) 15252.

values of the same parameters under different surface processing conditions, Fig. 3, indicate that they all measure *effective* lifetimes. It was shown that differences in lifetime values among the three techniques are likely due to the manner in which they incorporate additional transport parameters to the effective lifetime, such as the role of surface recombination and excess minority carrier-wave concentration. The dynamic nature of frequency-scanned PCR, coupled with analytical quantitative interpretation of the signals, allows for the measurement of bulk recombination lifetime, ambipolar diffusion coefficient and front- and back-surface recombination velocities. This capability renders the PCR bulk lifetime a very useful effective value accounting for the